ELSEVIER

Polymer 41 (2000) 7993–8000

polymer

www.elsevier.nl/locate/polymer

Solution properties of poly(diphenoxyphosphazene) below the θ temperature obtained by SEC/MALLS

M.T.R. Laguna, E. Saiz, M.P. Tarazona*

Departamento de Química Física, Universidad de Alcalá, 28871 Alcalá de Henares, Spain

Received 12 January 2000; accepted 23 February 2000

Abstract

Dilute solution properties of poly(diphenoxyphosphazene), PDPP, in THF at 25°C have been studied by size exclusion chromatography, using simultaneously multiangle light scattering and differential refractive index detectors. The anomalous elution behavior and the dependence of the dimensions, i.e. radius of gyration, of the polymer on the molecular weight are discussed. Coefficients for the scaling law and unperturbed dimensions have also been calculated. Molecular Dynamics simulations of some model compounds were performed in order to analyze the conformational characteristics of the P–N–P and N–P–N pairs of skeletal bonds. The conformational model thus obtained indicates that the PDPP chain is mainly formed by sequences of about four skeletal bonds in the *trans* conformation separated by one bond in *cis*, with negligible incidence of *cis–cis* orientations. The chain thus generated is very rigid so that the characteristic ratio of the unperturbed dimensions C_N increases with the number of repeat units of the chain x, up to values as high as $x \approx 800$, reaching an asymptotic value of ca 30 when $x \rightarrow \infty$, in very good agreement with the experimental result.

Keywords: Solution properties; Size exclusion chromatography; Light scattering

1. Introduction

Measurement of properties of polyphosphazenes in dilute solution is a powerful tool for both the characterization of these polymers and the study of their anomalous solution behavior. One of the problems frequently encountered in these measurements is the large polydispersity of the polymer samples due to the difficulties observed in the fractionation techniques when they are applied to poly phosphazenes [1]. Thus, the molecular weight dependence of properties such as radius of gyration can be masked by the discrepancies between the different molecular weight averages used. Different polydispersity corrections or numerical procedures have been used in order to solve the problem [2].

On the other hand, the use of a widely employed technique, size exclusion chromatography (SEC) for the solution characterization of polyphosphazenes has the inconvenience that the reliability of the universal calibration technique [3] becomes questionable for these polymers. Both problems can be surmounted using coupled multi-angle light scattering (MALLS) and refractometric (DRI) detectors in SEC measurements [4,5]. This experimental setup allows absolute distributions for both molecular weight and root mean square radius of gyration for polyphosphazenes from which information about their scaling law, $\langle s^2 \rangle^{1/2} = QM^q$, and unperturbed dimensions, $\langle s^2 \rangle_0^{1/2}$ and C_N, can be deduced [6].

We have applied these methods to several copolymers of polyphosphazenes containing spiro groups [7] finding that the logarithmic plots of the scaling laws show a pronounced curvature at low molecular weights. This peculiar behavior has also been encountered in other polymeric structures [8,9]. Thus, it seemed interesting to study the behavior of a simpler homo polyphosphazenes, i.e. poly(diphenoxyphosphazene), PDPP, and to compare the additional information obtained using this technique with previous literature results. Singler et al. [10] used viscosity and light scattering measurements to characterize a sample with broad molecular weight distribution ($M_n = 1.3 \times 10^5$, $M_w = 6.07 \times 10^5$, $M_w/M_n = 4.7$) in THF solution at 30°C. The behavior of the polymer in THF solution was indicative of near θ conditions. The low values of the second virial coefficient, A_2, together with the observed incipient precipitation as the polymer concentration was raised, or the temperature lowered, suggested that THF was a poor solvent for the polymer. They also found an important feature of dimensions which appears in others polyphosphazenes: the

* Corresponding author. Tel.: + 34-91-885-4664; fax: + 34-91-885-4763.

E-mail address: mpilar.tarazona@uah.es (M.P. Tarazona).

0032-3861/00/$ - see front matter
PII: S0032-3861(00)00169-5

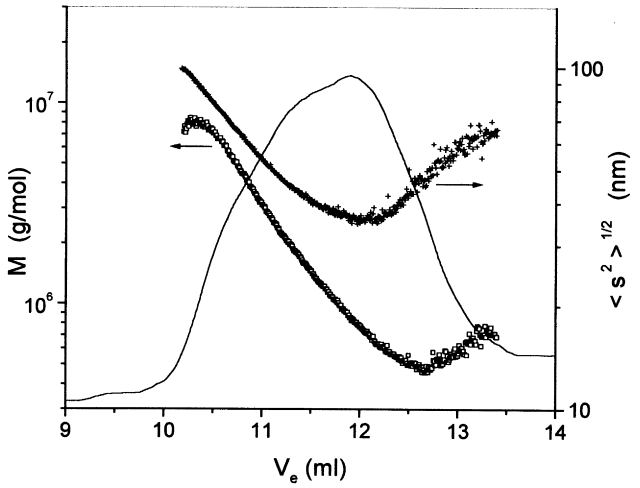

Fig. 1. Logarithm of molecular weight and root mean squared radius of gyration versus elution volume. The differential refractive index signal, in arbitrary units, is also shown.

differences between dimensions obtained by light scattering ($C_N = 54$) and viscosity ($C_N = 20$) measurements [11,12].

2. Experimental

A Waters Associates differential refractive index detector Model 410, was used as a concentration detector and a Dawn-DSP-F laser photometer from Wyatt Technology Corp. was used as the mass and size detector. A Model 510 pump, a U6K injector (Waters Associates) and two columns PLgel mixed B (Polymer Laboratories) in series completed the equipment. Tetrahydrofuran (THF) freshly distilled from sodium and benzophenone, filtered through a 0.2 μm Fluoropore filter and degassed, with a 0.1% tetra-*n*-butyl ammonium bromide was used as eluent at a flow rate of 1.0 ml/min. Poly(diphenoxyphosphazene) (supplied by Aldrich) was dissolved in THF and precipitated into methanol.

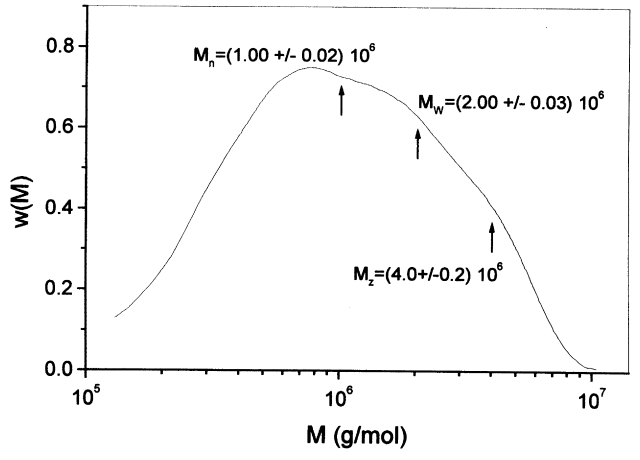

Fig. 2. Differential molecular weight distribution and molecular weight averages of the PDPP sample.

The Dawn photometer was calibrated with spectrometric grade toluene, freshly distilled from sodium and benzophenone, and the normalization of the detectors was performed with standard monodisperse polystyrene of low-molecular weight, which did not show angular dependence on the light scattering signal. Standard monodisperse polystyrene was also used to determine the inter-detector volume using the "spider" plot method [4]. A temperature of 25°C was used.

The Dawn photometer was also used for the batch measurements of light scattering of different concentrations of the polymer in order to obtain the value of the second virial coefficient. The solvent and temperature used were the same in the SEC measurements.

The OPTILAB DSP interferometric refractometer from Waters Associates Corp. was used for measuring the differential refractive index increment, d*n*/d*c*, of the polymer in THF, at a wavelength of 633 nm and a temperature of 25°C. A value of d*n*/d*c* = (13.09 ± 0.07) 10^{-2} ml/g was obtained.

^{31}P NMR spectrum was obtained with a UNITY 300 MHz. A single peak at 13.13, reported in ppm relative to H_3PO_4, was obtained ensuring that no branching occurred.

3. Results

The use of a multiangle light scattering detector allows us to calculate the weight average molecular weight and the root mean square radius of gyration $\langle s^2 \rangle^{1/2}$ for each slice across a sample peak of the SEC. Assuming that each slice contains molecules of a single molecular weight, or at least a very narrow distribution, a value of M is obtained for each elution volume. Fig. 1 shows this molecular weight, calculated from the scattered light, plotted versus the elution volume, i.e. absolute calibration curve for SEC together with the elution profile obtained by the differential refractive index detector. The molecular weight decreases as the elution volume increases until a point is reached from which the molecular weight starts to increase. Fig. 1 also shows the values of the root mean square radius of gyration [13], $\langle s^2 \rangle^{1/2}$, calculated from the angular dependence of the intensity of the scattered light, as a function of the elution volume. This magnitude provides an excellent representation of the polymer dimensions. As can be seen in the figure, the size of PDPP diminishes as the elution volume increases, in accordance to the SEC separation mechanism, until it reaches a point at which it starts to increase in a similar manner than that of molecular weight. The results are consistent in the range between 10 and 13.5 ml; out of this region, the signals from the detectors are too feeble and the dispersities of the points very large. The accuracy of the radius of gyration obtained in the region of high elution volumes (>12 ml) is lesser than that of molecular weight

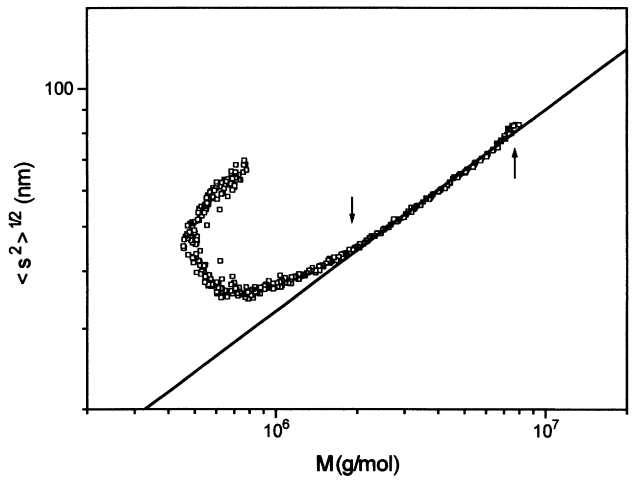

Fig. 3. Log–log plot of root mean squared radius of gyration versus molecular weight.

since the size of the polymer should be larger than $\lambda/20$ in order to notice the angular dependence of scattered light.

The combined measurements of molecular weight, obtained with the MALLS detector, and concentration, obtained with a differential refractive index detector, for each elution volume, allows to determine the absolute molecular weight distributions for the polymer samples [5]. Fig. 2 presents the absolute molecular weight distribution of the polymer and mean values of molecular weights. A polydispersity ratio $M_w/M_n = 2.0$ is obtained.

4. Discussion

The anomalous curvatures found for both the absolute molecular weight and the dimensions calibration curves of Fig. 1 are similar to our previous results for the spiro polyphosphazenes [7]. The increase in radius of gyration and the corresponding increase in molecular weight at high elution volumes, pointed above, can explain why the polyphosphazenes do not always follow the universal calibration assumptions [3] and also the difficulties usually found in the fractionation of these polymers [1].

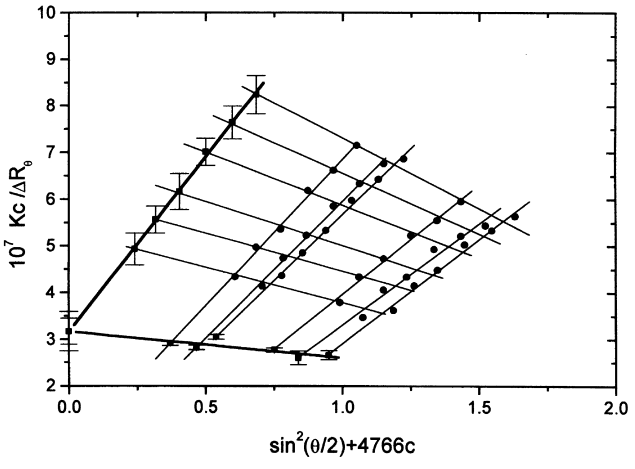

Fig. 4. Zimm plot of the PDPP sample.

4.1. Scaling laws

The study of the dependence of radius of gyration on molecular weight can give additional information on the polymer structure. Thus, the value of the q parameter in the scaling law $\langle s^2\rangle^{1/2} = QM^q$ may provide a hint about the conditions of the polymeric chain, since values of $q \simeq 0.5$ would indicate theta conditions and $0.5 < q \leq 0.6$ are obtained for random coil polymers in good solvents [14]. Fig. 3 shows the log–log plot of the simultaneously determined radius of gyration and molecular weight for the different slices of the PDPP chromatogram. The anomalous elution profiles found for PDPP (Fig. 1) lead to a non-linear relationship and the plot shows a pronounced curvature at low molecular weights.

Thus, there are two different values of the radius of gyration for the same molecular weight or, conversely, two different values of the molecular weight exhibit the same radius of gyration. Such an anomalous plot, similar to those obtained for other polyphosphazenes [7] have been observed for polystyrene microgels [4] and, recently, for stiff polymers with dendritic coats [8] and PMMA polymacromonomers [9]. The anomaly is qualitatively explained [8,9] by the existence of a small fraction of very large molecules which are retarded through the SEC columns, due to their size or molecular architecture, and elute at higher elution volumes, V_e, than the expected by a normal SEC mechanism. It is interesting to notice that the curvature appears earlier (i.e. at lower values of V_e) for $\langle s^2\rangle^{1/2}$ than for M. The reason may be that $\langle s^2\rangle$ is a z-average and therefore should be more sensitive to contamination with highly large molecules than the w-average M_w.

Linear regression at high molecular weights where the plot is linear (until the arrow in Fig. 3) yields the corresponding values $q = 0.435 \pm 0.003$ and $Q = 0.081 \pm 0.003$ for the scaling law coefficients. It is noteworthy to realize that curvature appears if the range is expanded towards lower molecular weights and thus the values obtained for Q and q depend on the chosen range of molecular weights. The values of the q parameter show that the polymer is slightly under θ conditions in good accord with the conclusions obtained by Singler et al. [10], who even noticed incipient precipitation of the polymer. In order to prove the poor solvent condition, light scattering measurements of solutions of different concentrations were performed. The Zimm plot is presented in Fig. 4. The plot does not show any curvature and from the slope of the extrapolation at zero concentration, a value of $A_2 = (-1.7 \pm 0.6)10^{-4}$ mol ml g^{-2} is obtained. This value corresponds to a polymer under θ conditions.

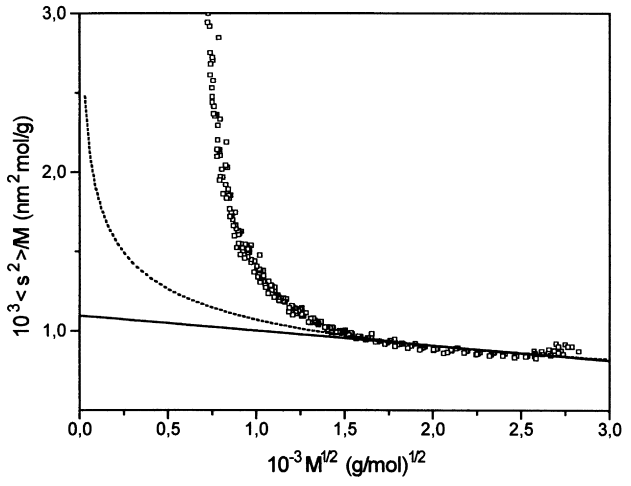

Fig. 5. Dependence on molecular weight of the experimental $\langle s^2\rangle/M$ ratio. The solid line shows the extrapolation to unperturbed dimensions. The broken line shows the calculated values using the scaling law.

4.2. Unperturbed dimensions

The perturbed and unperturbed mean square radius of gyration are related though the chain expansion factor, α:

$$\langle s^2\rangle = \alpha^2\langle s^2\rangle_0. \tag{1}$$

Recently [6], we have devised a procedure to obtain unperturbed dimensions from SEC/MALLS measurements of one sample of the polymer in a good solvent, using several extrapolation procedures. One, due to Fixman [15] is defined in Eq. (2), and affords $\langle s^2\rangle_o/M$ as the intercept:

$$\frac{\langle s^2\rangle}{M} = \frac{\langle s^2\rangle_0}{M} + 0.0299B\left(\frac{\langle s^2\rangle_0}{M}\right)^{-1/2} M^{1/2}. \tag{2}$$

However, THF is not a good solvent for PDPP and since, in this case, the polymer is near θ conditions the expression for the expansion coefficient given by the two parameters theory [16] may be used instead:

$$\alpha^2 = (1 + 1.276z - 2.082z^2 + \cdots) \tag{3}$$

and

$$\frac{\langle s^2\rangle}{M} = \frac{\langle s^2\rangle_0}{M}(1 + 1.276z - 2.082z^2 + \cdots) \tag{4}$$

where z is a parameter proportional to $M^{1/2}$ and to the excluded volume interaction energy of the polymer system, β.

Thus, the values of $\langle s^2\rangle/M$ versus $M^{1/2}$ should fit a polynomial:

$$\frac{\langle s^2\rangle}{M} = \frac{\langle s^2\rangle_0}{M}(1 + AM^{1/2} + BM + \cdots) \tag{5}$$

with $\langle s^2\rangle_0/M$ as the independent term. Eq. (5) is similar to Eq. (2) if only the first two terms of the polynomial are used. Fig. 5 shows the experimental values of $\langle s^2\rangle/M$ versus $M^{1/2}$ for the polymer. As explained above, there is a fraction of very large molecules, which are retarded through the SEC columns, causing the anomalous behavior of the scaling law at high elution volumes. The broken line in Fig. 5 represents the scaling law: $\langle s^2\rangle^{1/2}$ scales with $M^{0.43}$, so the ratio $\langle s^2\rangle/M$ will scale with $M^{-0.14}$. Thus, only experimental points that follow the scaling law are taken into account for the linear extrapolation, represented by the solid line in the same figure. A value of $\langle s^2\rangle_0/M = (1.13 \pm 0.01)10^{-3}$ nm^2 mol g^{-1} is obtained.

The negative slope exhibited by the extrapolation (Fig. 5) may seem surprising since extrapolations to unperturbed dimensions, performed with values measured in good solvents, usually show downwards curvature. However, it is a straight consequence of the under-θ conditions of the system i.e.: the value of α should decrease below unity [17]. Indeed, as it is indicated above, the ratio $\langle s^2\rangle/M$ will scale with $M^{-0.14}$ and will increase with decreasing M. The same kind of behavior is exhibited by other polymers and a good example is provide by the work of Li et al. [18] who measured light scattering of poly(α-methyl styrene) in cyclohexane solutions at θ conditions ($\theta = 36.2$°C) and below. Plots of their results at $T < \theta$ show the same type of curvature than our Fig. 5 and extrapolate to values of $\langle s^2\rangle_0/M$ which are virtually identical to those obtained by direct measurement at $T = \theta$.

It is also interesting to notice that, since we are so close to θ conditions, the experimental values of $\langle s^2\rangle/M$ for the different molecular weights (Fig. 5) scarcely vary between 0.8 and 1.0 in 10^{-3} nm^2 mol g^{-1}. As pointed above, the difficulties encountered in the fractionation of polyphosphazenes yield samples of large polydispersities which can mask the small dependence of $\langle s^2\rangle/M$ versus M if traditional methods, such as the measurements of a few samples obtained by fractionating the parental polymer, are used. Nevertheless, the greater sensibility of the SEC/MALLS measurements affords to study this dependence.

The characteristic ratio C_N can be calculated from the extrapolated value of $\langle s^2\rangle_0/M$ as:

$$C_N = \frac{\langle r^2\rangle_0}{Nl^2} = \frac{6M_0}{2l^2}\frac{\langle s^2\rangle_0}{M} \tag{6}$$

where N is the number of skeletal bonds, M_0 is the molecular weight of the repeating unit which contains two bonds P–N of length $l = 0.157$ nm, and $\langle r^2\rangle_0$ the unperturbed value of the mean square end to end distance, which for flexible chains is $\langle r^2\rangle_0 = 6\langle s^2\rangle_0$. The calculated value of C_N is 32.

We conclude that PDPP in THF solutions is slightly below θ conditions at 25°C. The SEC chromatogram of this system present upwards curvatures of both M and $\langle s^2\rangle^{1/2}$ versus V_e in the region of low-molecular weight that produce a hook-like plot of $\langle s^2\rangle^{1/2}$ versus M. The same kind of behavior has been reported for other systems. Combination of MALLS and DRI detectors on the SEC setup allows working with virtually monodisperse samples and therefore provide reliable values for the coefficients of

Table 1
Statistical weights, normalized to *trans–trans* N–P–N state, for the U_{PNP} and U_{NPN} matrices representing the conformational states allowed to the P–N–P and N–P–N pairs of skeletal bonds in PDPP

Statistical weight	Energy	Conformation	Interaction	Order
ω	E_ω	*tt* in P–N–P	OPh···OPh	Second
ω_1	$E_{\omega 1}$	*ct* or *tc* in P–N–P	N···OPh	Second
ω_2	$E_{\omega 2}$	*tt* in P–N–P	N···N	Second
ω_3	$E_{\omega 3}$	*ct* or *tc* in N–P–N	N···P	Second
ω_4	$E_{\omega 4}$	*tt* in N–P–N	P···P	Second

the scaling law and the extrapolation to unperturbed conditions.

4.3. Theoretical calculations

Values of the characteristic ratio C_N of PDPP were calculated with the statistical model recently developed for poly(dichlorophosphazene) [19]. In brief, this model employs two main rotational isomers (*cis* for $\phi = 0$ and *trans* for $\phi = 180$) for the P–N skeletal bonds. Taking the isomers in the order *cis*, *trans*, the statistical weight matrices for the two pairs of bonds appearing in the polymeric chain may be written as:

$$U_{PNP} = \begin{bmatrix} \omega_2 & \omega_1^2 \\ \omega_1^2 & \omega^2 \end{bmatrix} \qquad U_{NPN} = \begin{bmatrix} \omega_4 & \omega_3 \\ \omega_3 & 1 \end{bmatrix} \tag{7}$$

where the *trans–trans* state for the N–P–N pair of bonds was taken as reference. The ω's statistical weights are Boltzmann exponential of their corresponding energies which are summarized in Table 1.

Molecular Dynamics simulations were carried out for the two molecules represented in Fig. 6 which were assumed to stand alone in vacuo and employed as model compounds for the evaluation of the interactions that produce the conformational energies summarized in Table 1 as well as the averaged values of the PNP and NPN skeletal bond angles. MD simulations were performed with the DL_POLY package [20] and the force field described earlier [19]. A time step $\delta = 1$ fs (i.e. 10^{-15} s) was employed for integration of the equations of motion. The temperature of the system was kept constant at $T = 300$ K while producing the data of interest by means of a Nose–Hoover thermostat [21] with a relaxation time of 500 fs. Coulombic forces were computed as the sum of interactions among partial charges assigned to every atom of the molecules. These charges were computed for the cyclic trimer, $[P(OPh)_2–N–]_3$, using the gaussian package [22] and the 6-311g** basis set. The dielectrical constant of the systems was assumed to be distant dependent. A typical MD run employed 10^5 integration steps in a thermostation cycle during which the molecule was slowly warmed up from 0 to 300 K. Once the molecule was equilibrated at the working temperature, the simulation was prolonged for 10^7 steps, thus covering a time span of 10 ns, recording the molecular geometry every 200 steps. The resulting 50,000 conformations were then examined in order to calculate the skeletal bond angles and the rotations over the P–N bonds.

Averaged values of the two skeletal bond angles were $\theta(NPN) = 119.1°$ and $\theta(PNP) = 140.8°$. Fig. 7 shows the probability distribution for the rotational angles over the skeletal bonds assuming that each bond is independent of all its neighbors. As this figure indicates, *cis* and *trans* are indeed the preferred states, with almost the same independent probability for both of them.

The distribution of a priori probabilities for the P–N–P and N–P–N pairs of bonds is represented, respectively, in Figs. 8 and 9. The top panels of these figures are contour maps that gives a good idea of the position of the maxima, while the lower panels are surface maps in which the relative height of each maximum is better appreciated. Adding up the probabilities around every maxima and normalizing

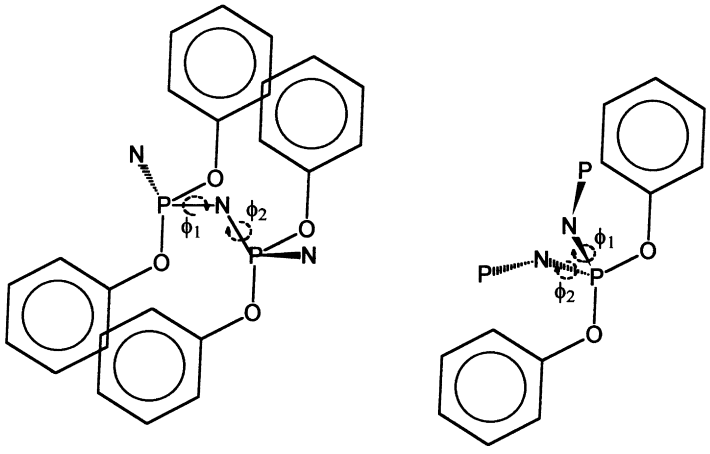

Fig. 6. Sketches of the $N–P(OPh)_2–N–P(OPh)_2–N$ and $P–N–P(OPh)_2–N–P$ molecules that were employed as model compounds to analyze the conformational characteristics of the P–N–P and N–P–N pairs of skeletal bonds.

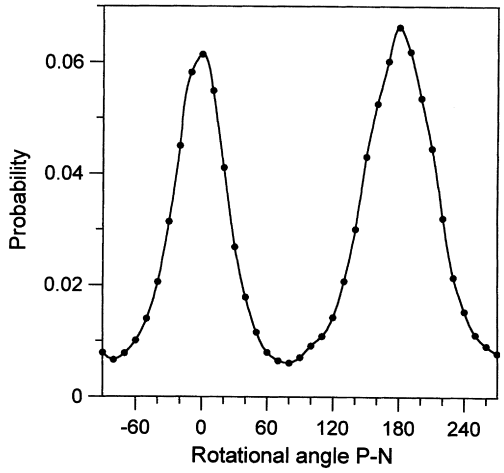

Fig. 7. Probability distributions for rotations over the skeletal bonds, computed at 300 K assuming that each bond is independent of all its neighbors.

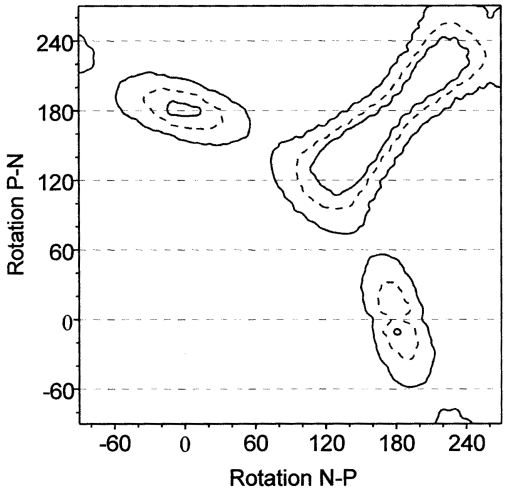

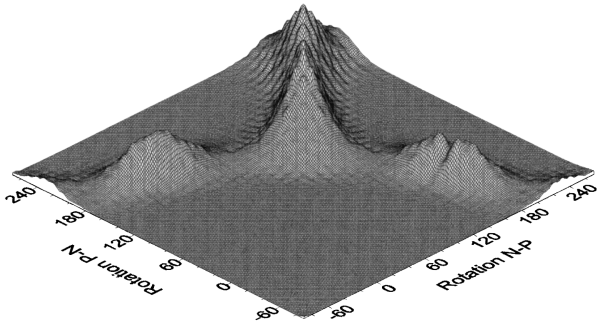

Fig. 9. Distribution of a priori probabilities computed at 300 K for the N–P–N pair of skeletal bonds in the P–N–P(OPh)$_2$–N–P molecule.

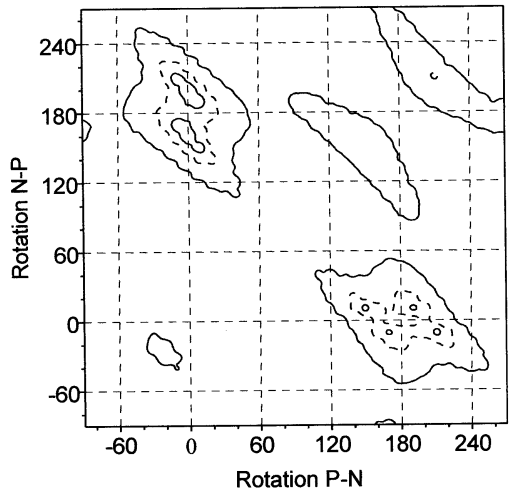

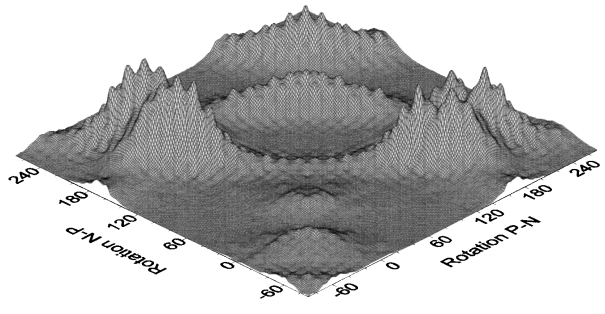

Fig. 8. Distribution of a priori probabilities computed at 300 K for the P–N–P pair of skeletal bonds in the N–P(OPh)$_2$–N–P(OPh)$_2$–N molecule.

the results, one obtains the following probabilities for the allowed orientations of each pair of bonds:

$$P_{\mathrm{PNP}} = \begin{bmatrix} 0.0782 & 0.3579 \\ 0.3579 & 0.2059 \end{bmatrix}$$
$$P_{\mathrm{NPN}} = \begin{bmatrix} 0.0000 & 0.1746 \\ 0.1746 & 0.6490 \end{bmatrix}. \tag{8}$$

These probabilities were computed for diads, which were alone, not surrounded by other diads of the chain. Therefore, after normalization with respect to tt conformation of the N–P–N pair of bonds, they should reproduce the statistical weight matrices given in Eq. (7). Thus:

$$U_{\mathrm{PNP}} = \begin{bmatrix} 0.1205 & 0.5515 \\ 0.5515 & 0.3173 \end{bmatrix}$$
$$U_{\mathrm{NPN}} = \begin{bmatrix} 0.0000 & 0.2690 \\ 0.2690 & 1.0000 \end{bmatrix}. \tag{9}$$

Taking into account that the calculations were performed at 300 K, the following values of conformational energies, in kcal/mol, are obtained: $E_\omega = 0.34$; $E_{\omega 1} = 0.18$; $E_{\omega 2} = 1.26$; $E_{\omega 3} = 0.78$; $E_{\omega 4} = \infty$.

However, although the main positions of the isomers for one isolated bond are *cis* and *trans*, Figs. 8 and 9 suggest that the actual position of some of the maxima are displaced by ca 40° from those main positions when pairs of bonds are considered. These displacements can be easily taken into account by splitting each isomer into three states, namely c_-, c, c_+, t_-, t, t_+ with values of the rotational angles $\phi = 180 - \Delta\phi$, 180, $180 + \Delta\phi$, $\Delta\phi$, 0, $\Delta\phi$ and $\Delta\phi$, $\approx 40°$. Writing the rotational isomers in this order, the statistical weight matrices will then be:

$$U_{\mathrm{PNP}} = \begin{bmatrix} \omega_2/2 & 0 & 0 & 0 & 0 & 0 \\ 0 & 0 & 0 & 0 & \omega_1^2 & 0 \\ 0 & 0 & \omega_2/2 & 0 & 0 & 0 \\ 0 & 0 & 0 & \omega^2/2 & 0 & 0 \\ 0 & \omega_1^2 & 0 & 0 & 0 & 0 \\ 0 & 0 & 0 & 0 & 0 & \omega^2/2 \end{bmatrix}$$

$$U_{\mathrm{NPN}} = \begin{bmatrix} \omega_4 & \omega_4 & \omega_4 & \omega_3 & \omega_3 & \omega_3 \\ \omega_4 & \omega_4 & \omega_4 & \omega_3 & \omega_3 & \omega_3 \\ \omega_4 & \omega_4 & \omega_4 & \omega_3 & \omega_3 & \omega_3 \\ \omega_3 & \omega_3 & \omega_3 & 1 & 1 & 1 \\ \omega_3 & \omega_3 & \omega_3 & 1 & 1 & 1 \\ \omega_3 & \omega_3 & \omega_3 & 1 & 1 & 1 \end{bmatrix} \tag{10}$$

Serial multiplication of these 6×6 matrices for a polymeric chain provides the same partition function and a priori probabilities for any sequence of states than the 2×2 matrices of Eq. (7).

The characteristic ratio of the unperturbed dimensions, $C_{\mathrm{N}} = \langle r^2 \rangle_0 / Nl^2$, was calculated with these six states matrices according to standard procedures of the matrix multiplication scheme [23–25]. Thus, chains containing up to $x = 800$ repeat units (i.e. $N = 2x = 1600$ skeletal bonds) were generated, the value of their mean squared end-to-end distance in unperturbed conditions $\langle r^2 \rangle_0$ was then computed and transformed into characteristic ratios employing a value of $l = 0.157$ nm for the P–N bond length. The results obtained at 300 K are shown in Fig. 10 which indicates that $C_{\mathrm{N}} \approx 30$ when $N \rightarrow \infty$, in very good agreement with the extrapolation to unperturbed conditions of the experimental results.

However, besides the point that both theory and experiment agree in obtaining a very large value of C_{N} for PDPP, much larger than poly(dichlorophosphazene) [19] for instance, Fig. 10 also illustrates another interesting feature of this polymer. Namely that the chain is very rigid so that C_{N} increases with x (or with N) even for very large chains and only reaches the asymptotic value for $N \rightarrow \infty$ at $x \approx 800$ repeat units while most synthetic polymers reach that limit for $x \approx 100$–200 units. This rigidity of the chain may be the reason why the extrapolation of experimental values

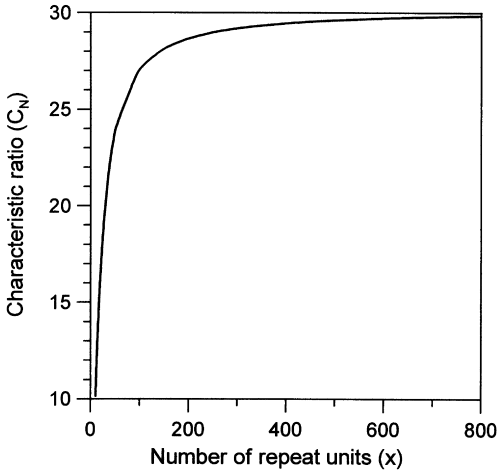

Fig. 10. Characteristic ratio of the unperturbed dimensions $C_{\mathrm{N}} = \langle r^2 \rangle_0 / 2xl^2$ as function of the number of repeat units in the chain, x. Calculations were performed at 300 K with the six states matrices. The P–N bond length was taken to be $l = 0.157$ nm. Skeletal bond angles $\theta(\mathrm{NPN}) = 119.1$ and $\theta(\mathrm{PNP}) = 140.8$ obtained by averaging the MD results were employed.

of $\langle r^2 \rangle$ or $\langle s^2 \rangle$ to unperturbed conditions departs from linearity unless extremely high-molecular weight samples are employed.

The reason for this rigidity and high dimension of the PDPP chain lies in the large preference of the skeletal bonds for *trans* states. Thus, the statistical weight matrices may be used to compute the a priori probability for a pair of P–N–P bonds within a long chain (for instance in the center of a chain containing $2x + 2$ repeating units), being in conformational state ij (with i and j representing *cis* or *trans*), as [23,24]:

$$p_{ij}(\mathrm{PNP}) = Z^{-1}[\,1 \quad 0][U_{\mathrm{PNP}}U_{\mathrm{NPN}}]^x U^0_{\mathrm{PNP}}\, U_{\mathrm{NPN}}[U_{\mathrm{PNP}}U_{\mathrm{NPN}}]^x \begin{bmatrix} 1 \\ 1 \end{bmatrix} \tag{11}$$

where the U^0_{PNP} matrix is obtained from U_{PNP} by replacing all its elements by zero except element ij which is left unchanged. Z is the partition function that can be obtained as [23,24]:

$$Z = [\,1 \quad 0][U_{\mathrm{PNP}}U_{\mathrm{NPN}}]^{2x+1} \begin{bmatrix} 1 \\ 1 \end{bmatrix}. \tag{12}$$

An equation similar to Eq. (12) with U^0_{NPN} instead of U^0_{PNP} can be used to compute p_{ij}(NPN). The results are:

$$P_{\mathrm{PNP}} = \begin{bmatrix} 0.0088 & 0.2005 \\ 0.2005 & 0.5902 \end{bmatrix}$$

$$P_{\mathrm{NPN}} = \begin{bmatrix} 0.0000 & 0.2093 \\ 0.2093 & 0.5814 \end{bmatrix} \tag{13}$$

and from them, the probability of *trans* replication, i.e. the probability of a *trans* bond being followed by another bond in *trans*, can be computed as [19]:

$$p_r = \frac{p_{tt}}{p_{tt} + p_{tc}} \approx 0.746. \quad (14)$$

Finally, the averaged length of *trans* sequences, i.e. the average number of skeletal bonds contained in all-*trans* sequences, is given by [19]:

$$\langle n_t \rangle = (1 - p_r) \sum_{i=1}^{\infty} i(p_r)^{i-1} = \frac{1}{1 - p_r} \approx 3.9. \quad (15)$$

Similar magnitudes for cis orientations give the values: $p_r(cis) \approx 0.042$ and $\langle n_c \rangle \approx 1.04$. Therefore, the chain contains sequences of about four skeletal bonds in all-*trans* conformation separated by one bond in *cis*, with negligible incidence of *cis–cis* conformations. Such an arrangement of rotational states produces a very rigid polymeric chain with high-unperturbed dimensions. These results may be compared for instance with those of poly(dichlorophosphazene) in which, depending of the conditions, $\langle n_t \rangle$ amounts to 2.7 or 1.7 producing values of $C_N \approx 15.7$ and 8.0, respectively [19].

We, therefore, conclude that the PDPP chain exhibits a strong preference for *trans* conformations that produces very high-molecular dimensions and a remarkable rigidity of the backbone.

Acknowledgements

This work was supported by the DGICYT through project PB97-0778. The assistance provided by Dr O. Castaño, who performed the ab initio calculations of the atomic partial charges, is gratefully acknowledged.

References

[1] Tarazona MP. Polymer 1994;35:819.
[2] Tarazona MP, Bravo J, Saiz E. Polymer Bull 1992;29:469.
[3] Grubisic Z, Rempp P, Benoit H. J Polym Sci Part B 1967;5:753.
[4] Wyatt PJ. Anal Chim Acta 1993;2721:1.
[5] Reed WF. In: Potschka M, Dubin PL, editors. Strategies in size exclusion chromatography, Washington, DC: American Chemical Society, 1996 (chap. 2).
[6] Búrdalo J, Medrano R, Saiz E, Tarazona MP. Polymer 1999;41:1615.
[7] Búrdalo J, Tarazona MP, Carriedo GA, García Alonso FJ, Gonzalez P. Polymer 1999;40:4251.
[8] Percec V, Ahn CH, Cho WD, Jamieson AM, Kim J, Leman T, Schmidt M, Gerle M, Möller M, Prokhorova SA, Sheiko SS, Cheng SZD, Zhang A, Ungar G, Yeardley DJP. J Am Chem Soc 1998;120:8619.
[9] Gerle M, Fischer K, Roos S, Müller AHE, Schmidt M. Macromolecules 1999;32:2629.
[10] Singler RE, Hagnauer GL, Schneider NS, Laliberte ER, Sacher ER, Matton RW. J Polym Sci Polym Chem Ed 1974;12:433.
[11] Pezzin G, Lora S, Busulini L. Polymer Bull 1981;5:543.
[12] Tarazona MP, Bravo J, Rodrigo MM, Saiz E. Polymer Bull 1991;26:465.
[13] Mattice WL, Suter UW. Conformational theory of large molecules. New York: Wiley, 1994.
[14] De Gennes PG. Scaling concepts in polymer physics. Ithaca, NY: Cornell University Press, 1979.
[15] Fixman M. J Chem Phys 1955;23:1656.
[16] Yamakawa H. Modern theory of polymer solution. New York: Harper and Row, 1971.
[17] Yamakawa H. Macromolecules 1993;26:5061.
[18] Li J, Harville S, Mays JW. Macromolecules 1997;30:466.
[19] Tarazona MP, Saiz E. Polymer 2000;41:3337.
[20] Forester TR, Smith W. DL_POLY (Ver. 2.10), Daresbury Laboratory, Daresbury, Warrington WA4 4AD, England.
[21] Allen MP, Tildesley DJ. Computer simulation of liquids. Oxford: Clarendon, 1987.
[22] Gaussian-94, Revision E.2, Gaussian, Inc., Pittsburgh PA, 1995.
[23] Flory PJ. Statistical mechanics of chain molecules. New York: Interscience, 1969.
[24] Flory PJ. Macromolecules 1974;7:381.
[25] Riande E, Saiz E. Dipole moments and birefringence of polymers. Englewood Cliffs, NJ: Prentice-Hall, 1992.